Mott-Hubbard Transition versus Anderson Localization in Correlated Electron Systems with Disorder

Krzysztof Byczuk,[1] Walter Hofstetter,[2] and Dieter Vollhardt[3]

[1]*Institute of Theoretical Physics, Warsaw University, ulica Hoża 69, PL-00-681 Warszawa, Poland*
[2]*Condensed Matter Theory Group, Massachusetts Institute of Technology, Cambridge, Massachusetts 02139, USA*
[3]*Theoretical Physics III, Center for Electronic Correlations and Magnetism, Institute for Physics, University of Augsburg, D-86135 Augsburg, Germany*

(Received 31 March 2004; published 10 February 2005)

The phase diagram of correlated, disordered electron systems is calculated within dynamical mean-field theory using the geometrically averaged (''typical'') local density of states. Correlated metal, Mott insulator, and Anderson insulator phases, as well as coexistence and crossover regimes, are identified. The Mott and Anderson insulators are found to be continuously connected.

DOI: 10.1103/PhysRevLett.94.056404 PACS numbers: 71.10.Fd, 71.27.+a, 71.30.+h

The properties of real materials are strongly influenced by electronic interaction and randomness [1]. In particular, Coulomb correlations and disorder are both driving forces behind metal-insulator transitions (MITs) connected with the localization and delocalization of particles. While the Mott-Hubbard MIT is caused by electronic repulsion [2], the Anderson MIT is due to coherent backscattering of noninteracting particles from randomly distributed impurities [3]. Furthermore, disorder and interaction effects are known to compete in subtle ways [1,4,5]. Several new aspects of this interplay are discussed here.

The theoretical investigation of disordered systems requires the use of probability distribution functions (PDFs) for the random quantities of interest. In physical or statistical problems one is usually interested in ''typical'' values of random quantities which are mathematically given by the most probable value of the PDF [6]. In many cases the complete PDF is not known; i.e., only limited information about the system provided by certain averages (moments or cumulants) is available. In this situation it is of great importance to choose the most informative average of a random variable. For example, if the PDF of a random variable has a single peak and fast decaying tails this variable is usually well estimated by its first moment, known as the *arithmetic* average. However, there are many examples, e.g., from astronomy, the physics of glasses or networks, economy, sociology, biology, or geology, where the knowledge of the arithmetic average is insufficient since the PDF is so broad that its characterization requires infinitely many moments. Such systems are said to be non-self-averaging. One example is Anderson localization: when a disordered system is near the Anderson MIT [3], most of the electronic quantities fluctuate strongly and the corresponding PDFs possess long tails [7]. At the Anderson MIT the corresponding moments might not even exist. This is well illustrated by the local density of states (LDOS) of the system. The arithmetic mean of this random one-particle quantity does not resemble its typical value at all. In particular, it is noncritical at the Anderson transition [8] and hence cannot help to detect the localization transition. By contrast, the *geometric* mean [9,10], which gives a better approximation of the most probable (typical) value of the LDOS, vanishes at a critical strength of the disorder and hence provides an explicit criterion for Anderson localization [3,11–13].

A nonperturbative theoretical framework for the investigation of correlated lattice electrons with a local interaction is given by dynamical mean-field theory (DMFT) [14,15]. If in this approach the effect of local disorder is taken into account through the arithmetic mean of the LDOS [16] one obtains, in the absence of interactions, the well-known coherent potential approximation [17], which does not describe the physics of Anderson localization. To overcome this deficiency Dobrosavljević and Kotliar [11] formulated a variant of the DMFT where the geometrically averaged LDOS is computed from the solutions of the self-consistent stochastic DMFT equations. Employing a slave-boson mean-field theory as impurity solver they investigated the disorder-driven MIT for infinitely strong repulsion off half filling. Subsequently, Dobrosavljević *et al.* [12] incorporated the geometrically averaged LDOS into the self-consistency cycle and thereby derived a mean-field theory of Anderson localization which reproduces many of the expected features of the disorder-driven MIT for noninteracting electrons. This scheme uses only one-particle quantities and is therefore easily incorporated into the DMFT for disordered electrons in the presence of phonons [18], or Coulomb correlations.

In this Letter we employ the DMFT with the typical LDOS to determine the nonmagnetic ground state phase diagram of the disordered Hubbard model at half filling for arbitrary interaction and disorder strengths. The system is described by a single-orbital Anderson-Hubbard model

$$H_{\mathrm{AH}} = -t \sum_{\langle ij\rangle\sigma} a_{i\sigma}^{\dagger} a_{j\sigma} + \sum_{i\sigma} \epsilon_i n_{i\sigma} + U \sum_i n_{i\uparrow} n_{i\downarrow}, \quad (1)$$

where $t > 0$ is the amplitude for hopping between nearest neighbors, U is the on-site repulsion, $n_{i\sigma} = a^\dagger_{i\sigma} a_{i\sigma}$ is the local electron number operator, $a_{i\sigma}$ ($a^\dagger_{i\sigma}$) is the annihilation (creation) operator of an electron with spin σ, and the local ionic energies ϵ_i are independent random variables. In the following we assume a continuous probability distribution for ϵ_i, i.e., $\mathcal{P}(\epsilon_i) = \Theta(\Delta/2 - |\epsilon_i|)/\Delta$, with Θ as the step function. The parameter Δ is a measure of the disorder strength.

This model is solved within DMFT by mapping it [15] onto an ensemble of effective single-impurity Anderson Hamiltonians with different ϵ_i:

$$H_{\mathrm{SIAM}} = \sum_\sigma (\epsilon_i - \mu) a^\dagger_{i\sigma} a_{i\sigma} + U n_{i\uparrow} n_{i\downarrow} + \sum_{\mathbf{k}\sigma} V_{\mathbf{k}} a^\dagger_{i\sigma} c_{\mathbf{k}\sigma} + V^*_{\mathbf{k}} c^\dagger_{\mathbf{k}\sigma} a_{i\sigma} + \sum_{\mathbf{k}\sigma} \epsilon_{\mathbf{k}} c^\dagger_{\mathbf{k}\sigma} c_{\mathbf{k}\sigma}. \quad (2)$$

Here $\mu = U/2$ is the chemical potential corresponding to a half-filled band, and $V_{\mathbf{k}}$ and $\epsilon_{\mathbf{k}}$ are the hybridization matrix element and the dispersion relation of the auxiliary bath fermions $c_{\mathbf{k}\sigma}$, respectively. For each ionic energy ϵ_i we calculate the local Green function $G(\omega, \epsilon_i)$, from which we obtain the geometrically averaged LDOS $\rho_{\mathrm{geom}}(\omega) = \exp[\langle \ln \rho_i(\omega) \rangle]$ [11,12,19], where $\rho_i(\omega) = -\mathrm{Im}\, G(\omega, \epsilon_i)/\pi$, and $\langle O_i \rangle = \int d\epsilon_i \mathcal{P}(\epsilon_i) O(\epsilon_i)$ is the arithmetic mean of O_i [20]. The lattice Green function is given by the corresponding Hilbert transform as $G(\omega) = \int d\omega' \rho_{\mathrm{geom}}(\omega')/(\omega - \omega')$. The local self-energy $\Sigma(\omega)$ is determined from the $\mathbf{k}$-integrated Dyson equation $\Sigma(\omega) = \omega - \eta(\omega) - 1/G(\omega)$, where the hybridization function $\eta(\omega)$ is defined as $\eta(\omega) = \sum_{\mathbf{k}} |V_{\mathbf{k}}|^2/(\omega - \epsilon_{\mathbf{k}})$. The self-consistent DMFT equations are closed through the Hilbert transform $G(\omega) = \int d\epsilon N_0(\epsilon)/[\omega - \epsilon - \Sigma(\omega)]$, which relates the local Green function for a given lattice to the self-energy; here $N_0(\epsilon)$ is the noninteracting DOS.

The Anderson-Hubbard model (1) is solved for a semi-elliptic DOS, $N_0(\epsilon) = 2\sqrt{D^2 - \epsilon^2}/\pi D^2$, with bandwidth $W = 2D$; in the following we set $W = 1$. For this DOS a simple algebraic relation between the local Green function $G(\omega)$ and the hybridization function $\eta(\omega) = D^2 G(\omega)/4$ holds [15]. The DMFT equations are solved at zero temperature by the numerical renormalization group (NRG) technique [21–24] which allows us to calculate the geometric average of the LDOS in each iteration loop. Alternatively, one can compute $\Sigma(\omega, \epsilon_i) = U\Gamma(\omega, \epsilon_i)$, where $\Gamma(\omega, \epsilon_i)$ is given by one- and two-point correlation functions [22], from which $G(\omega, \epsilon_i) = 1/[\omega - \epsilon_i - \Sigma(\omega, \epsilon_i) - \eta(\omega)]$ is obtained. This has the advantage of guaranteeing numerically exact NRG results at $U = 0$.

The main result of this Letter is the ground state phase diagram of the Anderson-Hubbard model at half filling shown in Fig. 1. Two different phase transitions are found to take place: a Mott-Hubbard MIT for weak disorder Δ and an Anderson MIT for weak interaction U. The two insulating phases surround the correlated, disordered metallic phase. The properties of these phases, and the transitions between them, are now discussed.

(i) *Metallic phase.*—The correlated disordered metallic phase is characterized by a nonzero value of $\rho_{\mathrm{geom}}(0)$, the spectral density at the Fermi level ($\omega = 0$). Without disorder DMFT predicts this quantity to be given by the bare DOS $N_0(0)$, as expressed by the Luttinger theorem [25]. This means that Landau quasiparticles are well defined at the Fermi level. The situation changes dramatically when randomness is introduced, since a subtle competition between disorder and electron interaction arises. Increasing disorder at fixed U reduces $\rho_{\mathrm{geom}}(0)$ and thereby decreases the metallicity as shown in the upper panel of Fig. 2. The opposite behavior is found when the interaction is increased at fixed Δ (see Fig. 3 for $\Delta = 1$); i.e., the metallicity improves in this case. In the strongly interacting metallic regime the value of $\rho_{\mathrm{geom}}(0)$ is restored, reaching again its maximal value $N_0(0)$. Physically this means that in the metallic phase sufficiently strong interactions protect the quasiparticles from their decay due to impurity scat-

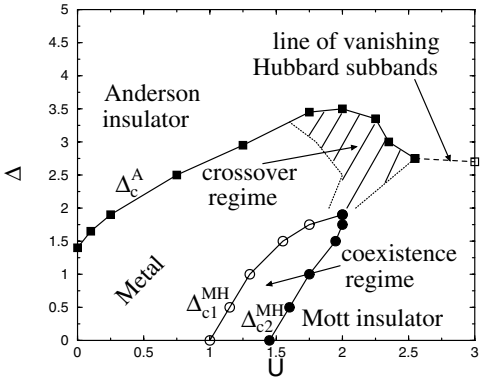

FIG. 1. Nonmagnetic ground state phase diagram of the Anderson-Hubbard model at half filling as calculated by DMFT with the typical local density of states.

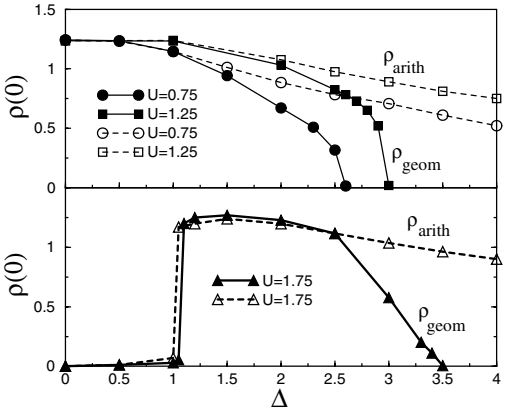

FIG. 2. LDOS as a function of disorder Δ for various values of the interaction U. Solid (dashed) curves correspond to the geometrically (arithmetically) averaged LDOS.

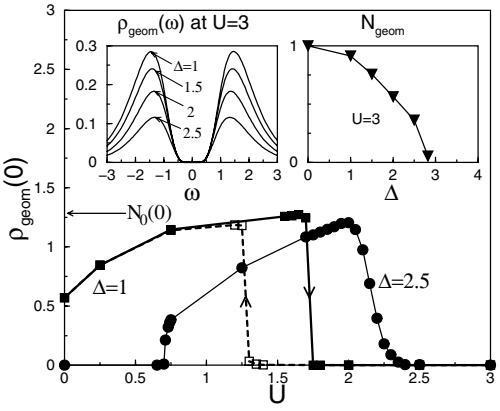

FIG. 3. Geometrically averaged LDOS as a function of interaction U for different disorder strengths Δ. Solid (dashed) curves with closed (open) symbols are obtained with an initial metallic (insulating) hybridization function. Triangles: $\Delta = 1$; dots: $\Delta = 2.5$. Left inset: LDOS with Mott gap at $U = 3$ for different disorder strengths Δ. Right inset: integrated LDOS N_{geom} as a function of Δ at $U = 3$.

tering. For weak disorder this effect of the interaction is essentially independent of the choice of the LDOS.

(ii) *Mott-Hubbard MIT.*—For weak to intermediate disorder there is a sharp transition at a critical value of U between a correlated metal and a gapped Mott insulator. We find two transition lines depending on whether the MIT is approached from the metallic side [$\Delta_{c2}^{\mathrm{MH}}(U)$, full dots in Fig. 1] or from the insulating side [$\Delta_{c1}^{\mathrm{MH}}(U)$, open dots in Fig. 1]. This is very similar to the case without disorder [15,23,26]; the hysteresis is clearly seen in Fig. 3 for $\Delta = 1$. The $\Delta_{c1}^{\mathrm{MH}}(U)$ and $\Delta_{c2}^{\mathrm{MH}}(U)$ curves in Fig. 1 have positive slope. This is a consequence of the disorder-induced increase of spectral weight at the Fermi level (see Fig. 4) which in turn requires a stronger interaction to open the correlation gap. In the Mott insulating phase close to the hysteretic region an increase of disorder will therefore drive the system back into the metallic phase. The corresponding abrupt rise of $\rho_{\mathrm{geom}}(0)$ is seen in the lower panel of Fig. 2 and the right column of Fig. 4. In this case the disorder protects the metal from becoming a Mott insulator.

Around $\Delta \approx 1.8$ the $\Delta_{c1}^{\mathrm{MH}}(U)$ and $\Delta_{c2}^{\mathrm{MH}}(U)$ curves terminate at a single critical point; cf. Fig. 1. At stronger disorder ($\Delta \gtrsim 1.8$) only a smooth crossover from a metal to an insulator takes place. This is clearly illustrated by the U dependence of $\rho_{\mathrm{geom}}(0)$ shown in Fig. 3 for $\Delta = 2.5$. In this parameter regime the Luttinger theorem is not obeyed for any U. In the crossover regime, marked by the hatched area in Fig. 1, $\rho_{\mathrm{geom}}(0)$ vanishes gradually, so that the metallic and insulating phases can no longer be distinguished rigorously [27].

(iii) *Anderson MIT.*—In Fig. 1 the metallic phase and the crossover regime are seen to lie next to an Anderson insulator phase where the LDOS of the extended states vanishes completely (see Fig. 4). The critical disorder $\Delta_c^A(U)$ corresponding to the Anderson MIT is a nonmonotonous function of the interaction: starting from the exact result $\Delta_c^A = e/2 \approx 1.36$ at $U = 0$ [12] it increases in the metallic regime and decreases in the crossover regime [28]. Where $\Delta_c^A(U)$ has a positive slope an increase of the interaction turns the Anderson insulator into a correlated metal. This is illustrated in Fig. 3 for $\Delta = 2.5$: at $U/W \approx 0.7$ a transition from a localized to a metallic phase occurs; i.e., the spectral weight at the Fermi level becomes finite. In this case the electronic correlations impede the localization of quasiparticles due to impurity scattering.

Figure 2 shows that the Anderson MIT is continuous. It should be stressed that an Anderson transition with vanishing $\rho_{\mathrm{geom}}(0)$ at finite $\Delta = \Delta_c^A(U)$ can be detected in DMFT only when the geometrically averaged LDOS is used (solid lines in Fig. 2). With arithmetic averaging one finds a nonvanishing LDOS at any finite Δ (dashed lines in Fig. 2).

(iv) *Mott and Anderson insulators.*—The Mott insulator with a correlation gap is rigorously defined only for $\Delta = 0$, and the gapless Anderson insulator only for $U = 0$ and $\Delta > \Delta_c^A(0)$. In the presence of interaction and disorder this distinction can no longer be made. However, as long as the LDOS shows the characteristic Hubbard subbands (see the left inset in Fig. 3) one may refer to a *disordered Mott insulator*. With increasing Δ the spectral weight of the Hubbard subbands vanishes (see the right inset in Fig. 3) and the system becomes a *correlated Anderson insulator*. The border between these two types of insulators is marked by a dashed line in Fig. 1. The results obtained here within DMFT show that the paramagnetic Mott and Anderson insulators are continuously connected. Hence, by changing U and Δ it is possible to move from one type of insulator to the other without crossing the metallic phase. This is possible because the Anderson MIT ($U = 0$) is not associated with the breaking of a symmetry [1].

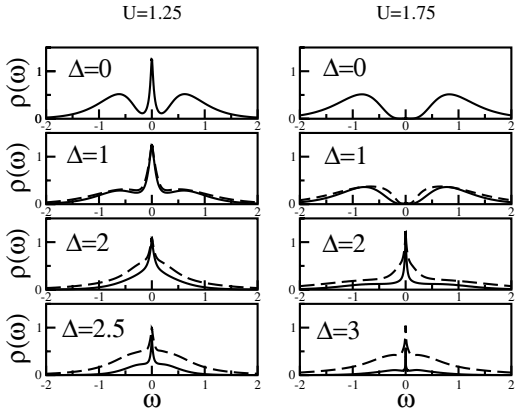

FIG. 4. LDOS for $U = 1.25$ (left column) and $U = 1.75$ (right column) for different disorder strengths Δ. Solid (dashed) curves correspond to the geometrically (arithmetically) averaged LDOS.

In conclusion, using DMFT with the geometrically averaged (typical) LDOS we computed the nonmagnetic ground state phase diagram of the Anderson-Hubbard model at half filling for arbitrary interaction and disorder strengths. In particular, we determined the position of the Mott-Hubbard metal insulator and Anderson localization transitions. The presence of disorder increases the critical interaction for the Mott-Hubbard MIT and turns the sharp transition (with hysteresis) into a smooth but rapid crossover. On the other hand, the critical disorder strength for Anderson localization increases for weak interaction and is suppressed by strong interactions. The paramagnetic Mott and Anderson insulators are continuously connected. The DMFT with geometric average can also be used to solve other correlated models. For example, we find that the phase diagram for the disordered Falicov-Kimball model has many features in common with those presented in Fig. 1. The specific predictions of our theory not only apply to disordered solids but also to cold fermionic atoms in optical lattices [29]. In the latter case a precise control of system parameters appears to be possible which, in principle, allows one to explore all parts of the phase diagram.

We thank R. Bulla, S. Kehrein, R. Kutner, D. Lobaskin, and J. Tworzydło for useful discussions. This work was supported in part by the Sonderforschungsbereich 484 of the Deutsche Forschungsgemeinschaft (DFG). K. B. acknowledges financial support through KBN-2 P03B 08 224, and W. H. through the DFG and an MIT Pappalardo grant.

[1] P. A. Lee and T. V. Ramakrishnan, Rev. Mod. Phys. **57**, 287 (1985); D. Belitz and T. R. Kirkpatrick, Rev. Mod. Phys. **66**, 261 (1994).

[2] N. F. Mott, Proc. Phys. Soc. London, Sect. A **62**, 416 (1949); *Metal-Insulator Transitions* (Taylor and Francis, London, 1990), 2nd ed.

[3] P. W. Anderson, Phys. Rev. **109**, 1492 (1958).

[4] S. V. Kravchenko *et al.*, Phys. Rev. B **50**, 8039 (1994); D. Popović, A. B. Fowler, and S. Washburn, Phys. Rev. Lett. **79**, 1543 (1997); S. V. Kravchenko and M. P. Sarachik, Rep. Prog. Phys. **67**, 1 (2004); H. von Löhneysen, Adv. Solid State Phys. **40**, 143 (2000).

[5] A. M. Finkelshtein, Sov. Phys. JETP **57**, 97 (1983); C. Castellani *et al.*, Phys. Rev. B **30**, 527 (1984); M. A. Tusch and D. E. Logan, Phys. Rev. B **48**, 14 843 (1993); **51**, 11 940 (1995); D. L. Shepelyansky, Phys. Rev. Lett. **73**, 2607 (1994); P. J. H. Denteneer, R. T. Scalettar, and N. Trivedi, Phys. Rev. Lett. **87**, 146401 (2001).

[6] The most probable value of a random quantity is defined as that value for which its PDF becomes maximal.

[7] A. D. Mirlin and Y. V. Fyodorov, Phys. Rev. Lett. **72**, 526 (1994); J. Phys. I (France) **4**, 655 (1994); M. Janssen, Phys. Rep. **295**, 1 (1998), and references therein.

[8] P. Lloyd, J. Phys. C **2**, 1717 (1969); D. Thouless, Phys. Rep. **13**, 93 (1974); F. Wegner, Z. Phys. B **44**, 9 (1981).

[9] *Log-Normal Distribution—Theory and Applications*, edited by E. L. Crow and K. Shimizu (Marcel Dekker, Inc., New York, 1988).

[10] E. W. Montroll and M. F. Schlesinger, J. Stat. Phys. **32**, 209 (1983); M. Romeo, V. Da Costa, and F. Bardou, Eur. Phys. J. B **32**, 513 (2003).

[11] V. Dobrosavljević and G. Kotliar, Phys. Rev. Lett. **78**, 3943 (1997).

[12] V. Dobrosavljević, A. A. Pastor, and B. K. Nikolić, Europhys. Lett. **62**, 76 (2003).

[13] G. Schubert, A. Weiße, and H. Fehske, cond-mat/0309015.

[14] W. Metzner and D. Vollhardt, Phys. Rev. Lett. **62**, 324 (1989).

[15] A. Georges *et al.*, Rev. Mod. Phys. **68**, 13 (1996).

[16] M. Ulmke, V. Janiš, and D. Vollhardt, Phys. Rev. B **51**, 10 411 (1995).

[17] R. Vlaming and D. Vollhardt, Phys. Rev. B **45**, 4637 (1992).

[18] F. X. Bronold, A. Alvermann, and H. Fehske, Philos. Mag. B **84**, 637 (2004).

[19] For a uniform PDF and N discrete values of ρ_i one finds $\rho_{\mathrm{geom}} = (\prod_{i=1}^{N} \rho_i)^{1/N} = \exp[(\sum_{i=1}^{N} \ln\rho_i)/N]$. Hence ρ_{geom} vanishes if any of the ρ_i is zero. The arithmetic average does not have such a property.

[20] For numerical integrations we use discrete values of ϵ_i selected according to the Gauss-Legendre algorithm [16].

[21] K. G. Wilson, Rev. Mod. Phys. **47**, 773 (1975); T. A. Costi, A. C. Hewson, and V. Zlatić, J. Phys. Condens. Matter **6**, 2519 (1994); W. Hofstetter, Phys. Rev. Lett. **85**, 1508 (2000).

[22] R. Bulla, A. C. Hewson, and Th. Pruschke, J. Phys. Condens. Matter **10**, 8365 (1998).

[23] R. Bulla, Phys. Rev. Lett. **83**, 136 (1999).

[24] The NRG method would be numerically exact for a discretization parameter $\Lambda = 1$ and broadening $b = 0$, but this would require infinite CPU time and memory. In our calculation we use $\Lambda = 1$ and $b = 0.55$.

[25] E. Müller-Hartmann, Z. Phys. B **76**, 211 (1989).

[26] M. J. Rozenberg, G. Kotliar, and X. Y. Zhang, Phys. Rev. B **49**, 10181 (1994).

[27] R. Bulla, T. A. Costi, and D. Vollhardt, Phys. Rev. B **64**, 045103 (2001).

[28] For $\Lambda > 1$ and $b > 0$ the NRG introduces small systematic errors in the numerical value of $\Delta_c^A(U)$ at large U but does not change its qualitative behavior.

[29] W. Hofstetter *et al.*, Phys. Rev. Lett. **89**, 220407 (2002); P. Horak, J. Y. Courtois, and G. Grynberg, Phys. Rev. A **58**, 3953 (1998); R. Roth and K. Burnett, J. Opt. B **5**, S50 (2003).